Available online at www.sciencedirect.com
ScienceDirect
Gene 391 (2007) 91–102
GENE
SECTION
FUNCTIONAL GENOMICS
www.elsevier.com/locate/gene

Dynamic changes in gene expression profiles of 22q11 and related orthologous genes during mouse development ☆

Francesca Amati [a,b,*], Michela Biancolella [a], Alessio Farcomeni [c], Stefania Giallonardi [a], Susana Bueno [c], Daniela Minella [a], Lucia Vecchione [a], Giovanni Chillemi [c], Alessandro Desideri [b,d], Giuseppe Novelli [a,b]

[a] *Department of Biopathology and Diagnostic Imaging, Tor Vergata University, Rome, Italy*
[b] *Interdisciplinar Centre for Bioinformatics and Biostatistics, Tor Vergata University, Rome, Italy*
[c] *CASPUR, Rome, Italy*
[d] *Department of Biology, Tor Vergata University, Rome, Italy*

Received 5 September 2006; received in revised form 30 November 2006; accepted 7 December 2006
Available online 19 January 2007
Received by R. Di Lauro

Abstract

22q11 deletion syndrome (22q11DS) is a developmental anomaly caused by a microdeletion on human chromosome 22q11. Although mouse models indicate that *Tbx1* is the gene responsible for the syndrome, the phenotypic spectrum of del22q11 patients is complex suggesting that gene–gene and gene–environment interactions are operative in delineating the pathogenesis of 22q11DS. In order to study the regulatory effects of 22q11 haploinsufficiency during development, the expression pattern of the orthologous MM16 genes was analysed in total embryos at different stages (from 4.5 dpc to 14.5 dpc; corresponding to pharyngeal development) by using a low-density oligonucleotide microarray (the "22q11DS-chip"). This microarray consists of 39 mouse genes orthologous to the 22q11 human ones and 29 mouse target genes selected on the basis of their potential involvement in biological pathways regarding 22q11 gene products.

Expression level filtering and statistical analysis identified a set of genes that was consistently differentially expressed (FC>±2) during specific developmental stages. These genes show a similar profile in expression (overexpression or underexpression). Quantitative real-time PCR analyses showed an identical expression pattern to that found by microarrays. A bioinformatic screening of regulative sequence elements in the promoter region of these genes, revealed the existence of conserved transcription factor binding sites (TFBSs) in co-regulated genes which are functionally active at 4.5, 8.5 and 14.5 dpc.

These data are likely to be helpful in studying developmental anomalies detected in del22q11 patients.

Keywords: Microarray; Time-course analysis; Regulation of gene expression; 22q11DS

1. Introduction

Deletion of the 22q11.2 chromosomal region causes the most common microdeletion syndrome in humans with an incidence of approximately 1:4000 live births (Scambler, 2000). The major malformations include congenital heart defects such as truncus arteriosus (TA) and interrupted aortic arch type B (IAA-B), hypo/aplasia of the thymus gland and craniofacial dysmorphism. However more than 180 clinical symptoms are due to 22q11 microdeletion (Ryan et al., 1997).

Although it has been demonstrated that many such phenotypic traits are due to changes in gene regulation of a

Abbreviations: 22q11DS, 22q11 deletion syndrome; FC, fold change; TFBSs, trasncription factor binding sites; DGS, DiGeorge syndrome; RA, retinoic acid.

☆ The data reported in this publication have been deposited in the NCBIs Gene Expression Omnibus (GEO, http://www.ncbi.nlm.nih.gov/geo/) and are accessible through GEO Series accession number GSE5050.

* Corresponding author. Via Montpellier 1, 00133 Rome, Italy. Tel.: +39 6 72596080; fax: +39 6 20427313.
E-mail address: amati@med.uniroma2.it (F. Amati).

0378-1119/$ - see front matter © 2007 Elsevier B.V. All rights reserved.
doi:10.1016/j.gene.2006.12.026

subset of genes mapping within the critical area (Lindsay and Baldini, 2001; Merscher et al., 2001; Jerome and Papaioannou, 2001; Epstein, 2001; Paylor and Lindsay, 2006), little is known concerning how this microdeletion acts on deregulating the expression of 22q11 genes. Identification of key genes involved in specific developmental processes requires an understanding of the patterns of gene expression in a specific tissue at a specific time. Microarray studies and transcriptional profiling experiments have revealed the involvement of newly discovered genes as well as providing a better understanding of the genetic pathways involved in embryo development in mouse models for the 22q11 deletion syndrome (Prescott et al., 2005; Ivins et al., 2005).

In this study, we evaluated the expression profile of the mouse orthologous genes in embryos at different developmental stages (from 4.5 dpc to 14.5 dpc), corresponding to the pharyngeal development. We used a low-density DNA microarray which includes both mouse genes orthologous to the human 22q11 region and genes considered to be putative "modifier genes" on the basis of their expression pattern and/or their interaction at a biochemical level with proteins encoded by 22q11 mapping genes.

2. Materials and methods

2.1. 22q11DS-chip

Microarrays are constructed by using oligonucleotide probes (50 mer, Ocimum Biosolutions, Indianapolis, USA), which are designed on the nucleotide sequence of the 3′ UTR of 68 genes. The 68 selected genes are 39 genes orthologous to human 22q11 ones and 29 genes mapping outside 22q11. These latter ones are genes involved in retinoic acid metabolism, in embryogenesis and genes already known to be "modifier" genes of the DGS phenotype (Table 1). We verified that each oligonucleotide probe was specific for the corresponding gene by using BLAST software (http://www.ncbi.nlm.nih.gov). Only for *Hira* gene, we decided to design two different oligonucleotide probes to recognize specifically the full-length cDNA and an alternative splicing form including exon 3a (Table 1). All the 68 oligonucleotides together with the positive controls were diluted in a spotting solution (Corning incorporated-Life Science, Acton, USA) at a final concentration of 50 pmol/μl. As positive controls of hybridization we used the oligonucleotides of Scorecard (Amersham Pharmacia Biotech, USA) and as negative controls we spotted only the spotting solution without oligonucleotides.

For array construction, each oligonucleotide probe is mechanically "spotted" onto UltraGAPS glass slides (Corning, USA) using The RoboArrayer™ (Microgrid Compact Plus, BioRobotics, Cambridge, UK). Each oligonucleotide probe is represented in triplicate per array. The printing conditions must be 50–55% humidity and a temperature of 25 °C. Printed slides are dried overnight and cross-linked with UV light at 600 mJ using a Strata-linker 2400 (Stratagene, Glenville, VA, USA). Finally, they are stored in a desiccator at room temperature. Before hybridization, each slide is incubated in a prehybridization buffer (5×SSC, 0.1% SDS, and 0.1 mg/ml BSA) at 42 °C for 45–60 min.

2.2. Preparation and hybridization of cDNA probes

Total RNA from mouse embryos at specific developmental stages is obtained by Seegene (Seegene Inc, Korea). Embryo samples from 4.5 dpc to 6.5 dpc include extra-embryonic tissues and maternal uterus, while samples from 7.5 dpc to 9.5 dpc are conceptuses, including embryo and extra-embryonic tissues. The samples from 10.5 dpc to 14.5 dpc are solely embryos. The RNA reference used in this study was obtained by pooling different CD1 mouse embryos at 18.5 dpc. The reference RNA was isolated by the TRIZOL standard protocol (Invitrogen Corporation, Carlsbad, USA). A small aliquot of RNA was then used for quantification and quality control by a spectrophotometer (Nanodrop, Wilmington, USA) and an agarose gel electrophoresis.

Synthesis of the labelled first strand cDNA was conducted using the Superscript Indirect cDNA labelling system (Invitrogen Corporation) with starting material of 10 μg of total RNA. The amino-allyl labelled dNTP mix was added to the reaction to generate amino-allyl labelled second strand cDNA. Following the hydrolysis reaction, single-stranded cDNA probes were purified using a Purification Module (Invitrogen Corporation). Probe mixtures where then evaporated in a vacuum centrifuge, and the cDNA pellet resuspended in 3 μl of water. The dye coupling reactions were performed by mixing the cDNA samples with AlexaFluor Dyes 555 or 647 and were incubated overnight in the dark. The reactions were purified with a Purification Module (Invitrogen Corporation) to remove the unincorporated/quenched dyes. After the purification, samples were combined for hybridization. The labelled cDNAs were co-hybridized to microarrays in duplicate, with one dye swap. The slides were scanned on the GenePix 4000B Microarray Scanner (Axon Instruments, Sunnyvale, USA) at the optimal wavelength for the Alexa555 (F532) and Alexa647 (F635) (Invitrogen Corporation) using lasers.

2.3. Image analysis and processing

The acquired images were analysed with GenePix Pro 5.0 (Axon Instruments). The oligonucleotide spots were automatically segmented; total intensities as well as the fluorescence ratios of the two dyes for each spot were then calculated. The spots were flagged when they exhibited poor hybridization signals, when they were saturated (F635 median = 65,535 or F532 = 65,535), or when their signal to background ratio was below two. We removed systematic bias in the data by applying the dye-swap normalization (Yang et al., 2001; Fang et al., 2003) in order to have the least possible information loss. Dye-swap normalization makes use of the reverse labelling in the two microarray replicates directly, and is particularly suitable for experiments in which a large number of the spotted genes are expected to change their expression level significantly. Correlations between raw intensity and background were computed for each spot; and background was not subtracted because of the low observed correlations, as suggested by Scharpf et al. (2005).

We compared the fluorescence for each gene at a specific developmental stage (i.e. 4.5 dpc) both against the reference

Table 1
The 68 genes that constitute the 22q11DS-chip with the accession number of the sequence chosen for oligonucleotide design and synthesis and the oligonucleotide sequences are indicated

Gene symbol	Accession number	Oligonucleotide sequence
Tbx1	NM_011532	TCTCCGCCGTGTCTAGTCCGTGGCTCACGCAGCTCTCGCACTTCTGCGAC
Gp1bB	NM_010327	CGGGCTGCTACACGCGCTGCTATTGGCACTTCTACTAGGTCGCCTGCGGA
Nogo-66	AF283462	CAGGAGGCCAGGTTGTTCCCGGAAGAATCGCACCCGCAGCCACTGCCGTC
Fgf8	NM_010205	CCAAACTACCCCGAGGAGGGATCTAAGGAACAGAGAGACAGTGTCCTGCC
Fgf10	NM_008002	ATACAACACCTATGCATCTTTTAACTGGCAGCACAATGGCAGGCAAATGT
Pax3	NM_008781	TCTCCCCTCTCACTGGGGGCCTGGAACCCACGACCACGGTGTCAGCCAGC
Ednra	XM_134499	GAACGAGTATCCAGTGGAAGAACCAAGAGCAGAACAACCACAACACGGAA
PLEXINA2	D86949	CTCGGACATCCATTAGCAGATATGACTCTTCCTTCAGGTACACAGGCAGC
Foxc1	NM_008592	GGATCGGCTTGAACAACTCCCCGGTGAATGGGAATAGTAGCTGTCAGATG
Foxc2	NM_013519	CTACGCCGTCCCTCTACCGCCACGCAGCCCCCTACTCTTACGACTGCACC
Sema3c	NM_013657	AGGGGACTATGGCAAGCTGAAGGCTCTCATCAACAGCAGGAAAAGCAGAA
Edn1	NM_010104	CAGCAATAGCATCAAGGCATCTTTTCGTGTTGCAAAGTTGAAAGCTGAGC
Pitx2	NM_011098	TCCGAAATCAAAAAGGTCGAGTTCACGGACTCTCCCAAGAGCCGGAAAGA
Shh	NM_009170	CTATGAATCCAAAGCTCACATCCACTGTTCTGTGAAAGCAGAGAACTCCG
Aldh1a2	NM_009022	AGTATTCAGAAGTAAAGACCGTGACGGTGAAGATCCCCCAGAAGAACTCC
Vegf	NM_009505	ACGTGTAAATGTTCCTGCAAAAACACAGACTCGCGTTGCAAGGCGAGGCA
Hoxa1	NM_010449	ACGTATAATAACTCCTTATCCCCTCTCCACGCCAGCCACCAAGAAGCCTG
Hoxb1	NM_008266	GGTCAAGAGAAACCCACCTAAGACAGCGAAGGTGTCCGAGCTGGGACTGG
Rarα	BC010216	TGGACACTCTAAGCGGACAGTCGGGGGGCGGAACACGAGATGGGGGTGGC
Rarβ	XM_127583	TCTGACTGACCTTGTGTTCACCTTTGCCAACCAGCTCCTGCCTTTGGAAA
Rarγ	BC013709	TGCCCGACAGCTACGAACTGAGTCCACAGTTAGAGGAACTCATCACCAAG
Rarx	NM_011305	ACCCAGGTGAACTCTTCGTCCCTCAACTCTCCAACGGGTCGAGGCTCCAT
Crabp1	NM_013496	GATCCGCCAAGACGGGGATCAGTTCTACATCAAGACATCCACTACTGTGC
Crabp2	M35523	CGAGAACTGACCAATGATGGAGAGCTGATCCTGACAATGACAGCAGATGA
Bmpr2	NM_007561	GCACTGCCACGACCACAGTGTCTAAAGATATAGGAATGAATTGTCTGTGA
Dvl2	NM_007888	AGCCTGGTGGGACTGGTGATGGCGGCCCTCCTCCATCCAGGGGCTCGACA
Hand2	NM_010402	GGGGCACCGCCAACCGCAAGGAGCGGCGCAGGACTCAGAGCATCAACAGC
Hcf2 (Serpind1)	NM_008223	GTGTACATAGGACTACATAGTCTATCCTAGAGATAAATAAACAACCATAT
Vpreb2	NM016983	GAGAATGGAGAGAGAGTGGGAAGGAGAAAAGTCGTATACAGATTTGGGAT
Vpreb1	NM016982	TATGAGCCCCCATTGGAGGCTGGATTGTAGAATTAAAGCTGTTTTTACTG
Lztr1	AK004561	GCTGGCTTGTGACTTTGTTTCCCGAGATACTGTAAAGAATATAAAGCCTA
Crkl	NM_007764	GCCTCCTTCTGCCTGTCAGTCTCCTTTGAAGTGGGAAGCACTCTGTCACA
Pcqap	AF328770	TCTGGTGAAAATTCCCCTTTTTATATGTGCACTACTCTGTCATATGATTC
Ube2l3	X97042	CAGGAACAGGGTGGTTTTCCCCTCCCTCTGGATTCCAAACCTTTCCAGTC
Idd/Dgcr2/Lan	NM_010048	ATTTCTAAGGTTTGGAGATTAAGCAAGGTTCTGTGCAATTTTTAGCACAT
Stk22a (Tsk1)	NM_009435	CTAAAGAAGCAATAAATCACTATATTGGTGCACACCCTAAAAAAAAAAAA
Tsk2 (Stk22b)	NM_009436	CATTAATTACTGACCACCAAATAAACCACAAAGTGTATACAAGTAAAAAA
Es2/Dgsi	NM_022408	TTCTAGCTAACCCCCAATTGAATCCTCATTAAAGAACACCTGGAACTGTC
CTP (SLC25A1)	AK005070	CTGTGAATATGTGCTCACTTATGCAATGCCTTGCTTGTGAGCCACATGCC
Dgcr6	AF021031	AATAAAGAACCCAGGACATGGTTTGTGTCTGTGCTACCTAGAAAAAAAAA
Prodh (hsPOX2)	NM_011172	AGGACAGACTAGGAAGCCTGTTTAGTCAATAAATCATCCTGTAACAGAGT
N41 (D22S1742E)	None	TTATGGCATGCGGCAAACACACAGTGCGCGGGTGGTGTAAGATAAACGAG
Htf9C	NM_008307	GGCCAGGACTGCCTAGCTGTACACCAGCTCTGCGCCCCCACTATGTCAAA
Ranbp1	NM_011239	TTTTGTTTTGTTTTTTTTTTAACTTTTTTTTACCTCCAAGTTTTGACACC
Arvcf	NM_033474	TGACAAAATGCATTAAAAATGAAACCAAAATAAGACTATCAACAAAAATT
Comt	NM_007744	GCAAAACCCCTCACGGTGAATCCTCTGCACCCAAGAACAAAAAGGGAGAT
Txnrd2	NM_013711	GCCAGCCTCTGACACTCCCAGCGTCAGATGATGATGGCCTGGGCAGAAAC
Gnb1l/Wdvcf	AF301595	AGACACCTGGCACCTATAGCTTGGTAACAGGCATGTTTTAGACCTGGTTG
Pnutl1 (hCDCrel-1)	AF033350	CCAGCAACTCTGTTGCACAAGGATTCCAGCCCTTGGCCTCCTCCATATCT
Cldn5 (Tmvcf)	NM_013805	TACTGAGATCCTGGGGGCACTAGATGCTGCCTTAATGTCCAGTGGCACCT
Cdc45l	AF098068	TCCTGGCCACTATTCAGTTGTAAGATAACATTTGAAATGTGAGACTATAT
Ufd1l	NM_011672	GTTCATGGTGCAGTGTCTTTAGCCCATCATGGCTACTCAGGCCAGCACTT
Nlvcf (cDNA FLJ33146)	NM_010922	GAGTCATCCTAGGAACAAATAAAGGGTAATCAAGAGTAAAAAAAAAAAAA
Hira	X99712	GCAGCTTGTCCCTCCATGTAGGCCCAGCTGTGGACTTGGGGCTGGGACTG
Hira (ex 3a)	X99713	GCCACGAACCATTTGGACGTCTGCGA
Atp6E	U13841	CATGCTGTCCCTGCTCTTTGGGCATAAAGTGCATGTGGGGACTCACATTC
Bid	NM_007544	CACTGGACATCTCTGCGTTCAGCTTGAGTGTATCTGAAGAGTTTACGCCG
Usp18	NM_011909	GCCTTCAAAATTCTGAATCTAATAAACATTAATGCACACTAAAAAAAAAA
Pik4CA	BC022127	CAATGGAAGAGGGGGCCGGTGCCAGGCCCAGTGGGCAAGGGTGCAGGCAG
cDNA homologous to Snap29 (rat)	NM_023348	TAATATAACGTGTTTTCAAATGTGGGTCTTTGAAATATTAGTTTCAATGG
P2rxl1	NM_011028	CGGGACTAGAGGGGAGTTGGGATAATTCCGACAGACTCCGAATGCAGATT
Top3b	NM011624	ATCTTTTCCCCACTCCAGACACATCGTGGTTATCTTTGAGCCACTGAAAC

(continued on next page)

Table 1 (*continued*)

Gene symbol	Accession number	Oligonucleotide sequence
Gnaz	AF056973	CCCGGGAACTGGAAAATAAGAATCTCTGAGTAGGGTTGCGGATGCCTGGA
Rab36	AK018269	CATGTTCCAAGCACCGAGACTTGTCAGAGGAAGCGAGTAAAACTAAAATG
Npl4	AA015556	GCCTTTAACCCTACCGAGGTCGATGTTTCCATTTCAGACGAG
p97	AF122047	CAGCTGCTTATAAACTAAGGAGCCAATCAATTGAAGCCAAGTAGGAGAGG
Dgcr8	NM_033324	GGGTTCACGGCTAAAGCAATCGTTCAAAGAGACAGAGTGGATGAAGAGGC
Hoxa3	Y11717	TGTTTTGTTCTATGTTCTTGCCTTTCCCTTTTCTCCTCTGCACCCCTCCC

(18.5 dpc pooled embryos) and against the following time frame (i.e. 4.5 dpc vs 6.5 dpc; time-course analysis).

Certainly, there is an intrinsic dependence in the data, given that each comparison was done between repeated measurements on the same tissue, at different times. This was taken directly into account by forming individual fold changes and performing a standard one-sample *T*-test on a log2 scale for each gene. We corrected for the multiplicity of testing by controlling the False Discovery Rate (FDR) of Benjamini and Hochberg (1995), in order to avoid a large number of false rejections. FDR control is different than common Type I error control. FDR control at level 0.05 implies that the expected number of genes which are erroneously declared significant divided by the number of selected genes (if any), is below 5%. For a discussion of the implications of controlling such an error measure see Farcomeni (in press).

2.4. Validation of relative gene expression by real-time RT-PCR

The total RNA was reverse-transcribed to cDNA according to the protocol of the High-Capacity cDNA Archive Kit (Applied Biosystems, Foster City, USA). The incubation conditions were the following: 10 min to 25 °C and 2 h to 37 °C. We performed quantitative real-time PCR (QRT-PCR) using the Taqman system (Applied Biosystems). The expression levels of four selected genes and an internal reference (*GAPDH*) were measured by multiplex PCR using Assay-on-Demand™ gene expression products (Applied Biosystems, Foster City, CA, USA) labelled with 6 carboxyfluorescein (FAM) or VIC (Applied Biosystems). We analysed the following genes: Mm00442776_m1 (*Crabp1*); Mm00546194_s1 (*Foxc2*); Mm00448948_m1 (*Tbx1*); Mm00465044_m1 (*Mrpl40*). The simultaneous measurement of each gene-FAM and GAPDH-VIC made it possible to standardize the amount of cDNA added per sample. We performed PCRs using the Taqman Universal PCR Master Mix and the ABI PRISM 7000 Sequence Detection System. Each QRT-PCR experiment was performed in triplicate and repeated at least twice. A comparative threshold cycle (C_T) was used to determine gene expression relative to a calibrator (RNA from pooled 18.5 dpc embryos). Hence, steady state mRNA levels are expressed as *n*-fold difference relative to the calibrator. For each sample, our C_T genes value is normalized using the formula $\Delta C = C_{tgene} - C_{tGAPDH}$. To determine relative expression levels, the following formula was used: $\Delta\Delta C_T = \Delta C_{Tsample} - \Delta C_{Tcalibrator}$ and the value used to plot relative gene expression was calculated using the expression $2^{-\Delta\Delta C}{}_T$.

2.5. Promoter analysis

We complemented the experimental study by analysing the regulatory signals in the aligned human and murine 5 kb region upstream the transcription start site, of the 11 co-regulated genes (in bold) (Table 2). The 5 kb human and murine regions were obtained from the UCSC Genome Bioinformatics Site (http://genome.ucsc.edu). Homologous human and murine sequences for each gene were aligned using the DiAlign program and potential transcription factor binding sites (TFBS) were searched using the MatInspector program which compares the input sequence against a large library of weight matrices with the complete nucleotide distribution for each single position (Cartharius et al., 2005).

3. Results

3.1. Gene expression pattern of 22q11DS-chip at each developmental stage

The gene expression levels of 68 genes was analysed by microarray technology (Table 1) in total RNA from embryos at different developmental stages (from 4.5 to 14.5 dpc). We performed experiments in duplicate using reverted labelled RNA. As a reference sample, we used the total RNA obtained from pooled 18.5 dpc mouse embryos (CD1 strain). This stage corresponds to the end of the embryonic development and so we have decided to compare the expression pattern of the selected 68 genes in embryos at different stages to the final stage of development. This means that those genes expressed only in a specific developmental stage or only in the control RNA are filtered (see Section 2.3). So, the results discussed above regard genes whose expression level is high or low compared to the final stage of development.

The raw expression data of all the experiments are available as a specific GEO Sample record and may be linked as follows: http://www.ncbi.nlm.nih.gov/geo/query/acc.cgi?acc=GSE5050.

After data normalization, statistically significant genes at each developmental stage were identified (Table 2).

At 4.5 dpc, a developmental stage corresponding to the attachment of blastocyst and in which there is the first evidence of embryonic endoderm cells covering the surface of the inner cell mass, a total of six transcripts were found to be expressed (8.8%). Three of them were expressed at a twofold level (*Pax3*, FC = −2.54; *Hoxa1*, FC = −2.66; *Foxc2*, FC = −3.16) (Table 2, in bold). None of them maps in the 22q11 chromosomal region.

At 6.5 dpc gastrulation starts and there is the first evidence of mesoderm. Thirteen genes (19.1%) were expressed; three of

Table 2
The significant expressed genes at each developmental stage analysed are shown

Gene	FC	*p*
Stage 4.5 dpc		
Pax3	**−2.5**	**0.0025**
Stk22a	1.44	0.0292
Hoxa1	**−2.7**	**0.00667**
Top3b	1.35	0.0117
Usp18	1.5	0.025
Foxc2	**−3.2**	**0.029**
Stage 6.5 dpc		
Pnutl1	−1.47	0.0037
Nogo66	−1.38	0.0148
Gnb1l/Wdvcf	−1.49	0.0045
Pcqap	1.32	0.0034
Ctp	1.52	0.0114
Stk22a (Tsk1)	**2.45**	**0.0005**
Hoxa1	−1.17	0.0445
Usp18	**2.25**	**0.0012**
Txnrd2	**2.33**	**0.0032**
Es2/Dgsi	1.23	0.0488
Ube2l3	1.87	0.0133
Rarb	−1.84	0.0439
Hoxa3	−1.53	0.0087
Stage 7.5 dpc		
Pnutl1	−1.15	0.0309
Pcqap	1.34	0.0071
Stk22a	1.79	0.0037
Top3b	1.11	0.0153
Usp18	**2.61**	**0.0008**
Cldn5 (Tmvcf)	1.43	0.0278
Atp6E	1.51	0.0019
Hoxa3	−1.84	0.0028
Stage 8.5 dpc		
Pax3	−1.42	0.0138
Hoxa1	1.27	0.0436
Mrpl40 (Nlvcf)	1.56	0.016
Foxc2	−1.86	0.0018
Txnrd2	**5.09**	**0.025**
***Cldn5* (Tmvcf)**	**2.53**	**0.0219**
Hoxa3	−1.72	0.0027
Stage 9.5 dpc		
Nogo66	−1.5	0.0043
Tbx1	−1.4	0.0255
Bmpr2	−1.5	0.0074
Foxc1	−1.9	0.0011
Pax3	−1.25	0.008
Crabp1	**6.1**	**0.0288**
Foxc2	−1.47	0.0048
Txnrd2	**2.27**	**0.0202**
Cldn5 (Tmvcf)	1.6	0.0051
Ube2l3	1.31	0.0009
Hoxa3	−1.93	0.0067
Stage 11.5 dpc		
Comt	**−2.3**	**0.0272**
Foxc2	1.94	0.0077
Stage 14.5 dpc		
Gnaz	1.21	0.0168
Nogo66	−1.4	0.026
Gnb1l/Wdvcf	−1.52	0.0106

Table 2 (*continued*)

Gene	FC	*p*
Stage 14.5 dpc		
Lztr1	1.41	0.0075
Ctp	1.27	0.0178
Bid	1.21	0.0342
Foxc1	1.43	0.0121
STk22a	1.71	0.0018
Idd/Dgcr2/Lan	1.7	0.0021
Mrpl40 (Nlvcf)	**2.34**	**0.0164**
Ranbp1	**2.13**	**0.0021**
Usp18	1.66	0.016
Foxc2	1.21	0.0125
Txnrd2	−1.54	0.0027
Cldn5 (Tmvcf)	−1.63	0.007
Es2/Dgsi	−1.12	0.0264
Atp6E	−1.37	0.0035
Ube2l3	1.66	0.0017
Hoxa3	−1.31	0.0007

Genes expressed with a FC>±2 are indicated in bold.

them have expression levels >+2 (*Stk22a*, FC=+2.45; *Usp18*, FC=+2.25; *Txnrd2*, FC=+2.33) (Table 2, in bold). These genes map in the 22q11 typically deleted region (TDR; Scambler, 2000).

At 7.5 dpc embryos are characterized by neural plate formation; moreover, they develop the head process. Eight genes were expressed (11.8%), but only one was found expressed at a twofold level (*Usp18*, FC=+2.61) (Table 2, in bold).

At 8.5 dpc, the embryo turns, the first branchial arch has maxillary and mandibular components, and a second branchial arch becomes evident. There is evidence of regionalisation of the heart and the neural tube is closed from a point opposite the outflow tract to the proximal part of the tail. At 8.5 dpc seven genes were expressed (10.3%). Two of them were over-expressed: *Txnrd2* (FC=+5.09) and *Cldn5* (FC=+2.53) (Table 2, in bold) and both map in the TDR.

At 9.5 dpc, the third branchial arch is visible. Moreover, embryos show formation of the posterior neuropore. Eleven genes were expressed (16.2%) and two of them showed a twofold or more increase: *Crabp1* (FC=+6.1) and *Txnrd2* (FC=+2.27) (Table 2, in bold).

At 11.5 dpc, differentiation of the third pharyngeal arch begins. Only two genes were expressed (2.9%). One of them, *Comt* (FC=−2.29) showed a twofold level (Table 2, in bold).

At 14.5 dpc, embryos show fingers which are distally separated and the long bones of the limbs are present. Twenty-one genes were expressed (30.9%). Two of them were overexpressed, *Mrpl40* (FC=+2.34) and *Ranbp1* (FC=+2.13). Both genes map in the TDR (Table 2, in bold).

3.2. Expression of 22q11DS-chip genes during the entire pharyngeal development

To study the change of expression of the monitored 68 genes during all the developmental stages analysed, we compared the AlexaFluor Dyes 555/647 ratio of each gene at a specific

developmental stage to the following one (i.e. 4.5 dpc vs 6.5 dpc; time-course analysis). Using this approach, we detect possible genes that are differentially expressed in two subsequent stages. This approach also makes it possible to evaluate genes that are constantly expressed, i.e., that do not significantly change expression in two subsequent stages while being differentially expressed compared to the reference RNA (pooled 18.5 dpc embryos). Through this statistical analysis, we were able to identify genes expressed during the entire pharyngeal development.

Five genes, among the 68 genes analysed, were found to be significantly expressed after this time-course analysis (Fig. 1). Two of them are orthologous to those mapping within the 22q11 chromosomal region (*Mrpl40* and *Ranbp1*). Conversely, three map outside this region (*Foxc2*, *Pax3* and *Hoxa1*).

Among the genes orthologous to the 22q11 chromosomal region, *Ranbp1* is constantly expressed from 4.5 dpc to 11.5 dpc, then increases its expression at 14.5 dpc (Fig. 1A). *Mrpl40* shows a constant profile of expression from stage 4.5 dpc to stage 9.5 dpc, but at 11.5 dpc reduces its expression followed by an overexpression (Fig. 1B).

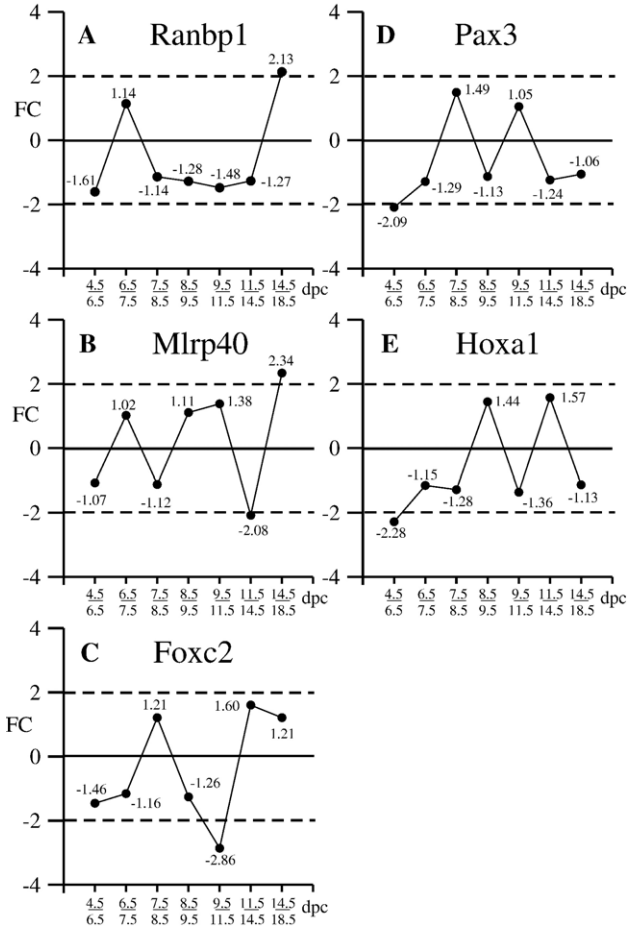

Fig. 1. The dynamic expression pattern of the five genes constantly present during pharyngeal development. Each FC is obtained by a comparison between the expression value at a developmental stage and the following one (i.e. 4.5 dpc vs 6.5 dpc; see also Materials and methods, Section 2.3).

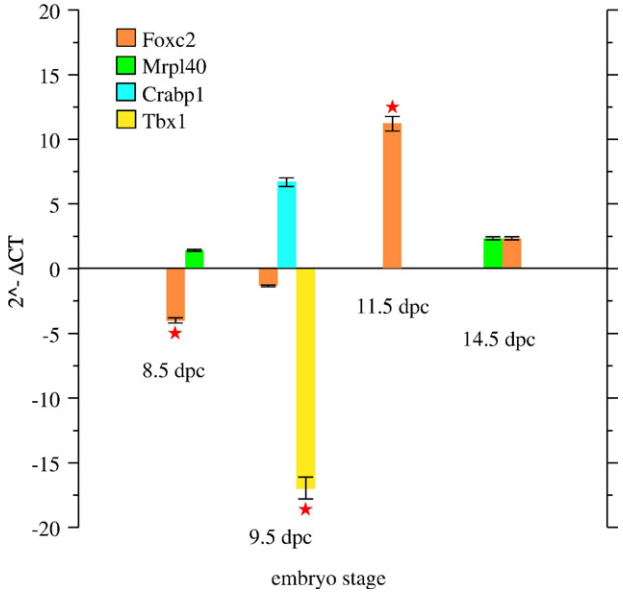

Fig. 2. Histograms represent the expression data obtained after QRT-PCR of some of the significant genes found after microarray analysis. Values indicated are the mean of at least two separate experiments performed in triplicate. Stars indicate the QRT-PCR expression values that are considerably greater than microarray values.

As regards the other three genes, *Foxc2* shows an under-expression at stage 9.5 dpc (Fig. 1C) while *Pax3* and *Hoxa1* are underexpressed at stage 4.5 dpc, but maintain a constant expression throughout 6.5 dpc to 14.5 dpc (Fig. 1D and E).

3.3. Validation of microarray gene expression data by QRT-PCR

We analysed the gene expression level of four genes, *Crabp1*, *Foxc2*, *Mrpl40* and *Tbx1*, by quantitative real-time PCR (QRT-PCR). The housekeeping gene *Gapdh* was used as an internal control. The mRNA expression values (ΔC_T) of *Crabp1*, *Foxc2*, *Mrpl40* and *Tbx1* genes during specific developmental stages (only the significant microarray values) are shown in Fig. 2. The results confirm the expression patterns seen with the low-density microarray (Table 2). However, we noticed that in three cases the QRT-PCR expression values are considerably greater than microarray values (Fig. 2, genes indicated by stars). Particularly impressive is the expression value of *Tbx1* at 9.5 dpc which was found to be intensely underexpressed (FC = −16.96; Fig. 2), whereas microarray analyses revealed a weak expression (FC = −1.38, Table 2).

3.4. Analysis of upstream genomic regions of 22q11DS-chip expressed at specific developmental stages

To search common and conservative potential transcription factor binding sites (TFBSs), we examined the 5 kb upstream genomic region of the 11 co-regulated mouse genes (Table 2, in bold). Firstly we aligned the 5 kb genomic region, upstream the transcription start site, of both human and mouse genes; after this, we analysed the conserved genomic sequences searching common TFBSs. We chose an optimized matrix

Table 3
Putative transcription factor binding sites (TFBSs) in the human and mice promoter region of the co-regulated genes, with respect to the developmental stage, are summarised

Developmental stage	Transcription factor	Score	Presence in the promoter region
4.5 dpc	Kruppel-like zinc finger protein 219	0.91	1
	Homeodomain transcription factor Gsh-2	0.95	2 (*Pax3* and *Foxc2*) 1 (*Hoxa1*)
	Cell cycle gene homology region	0.92	1
	Homeo domain factor Nkx-2.5/Csx	0.88	2 (*Pax3*) 1 (*Foxc2* and *Hoxa1*)
	Hmx2/Nkx5-2 homeodomain transcription factor	0.82	1 (*Pax3* and *Foxc2*) 3 (*Hoxa1*)
	PBX-HOXA9 binding site	0.79	1 (*Pax3* and *Foxc2*) 2 (*Hoxa1*)
	Myelin transcription factor 1-like	0.92	1 (*Pax3* and *Foxc2*) 2 (*Hoxa1*)
	Fork head related activator-2 (*FOXF2*)	0.84	1 (*Pax3* and *Foxc2*) 3 (*Hoxa1*)
	Signal transducers and activators of transcription	0.87	1
	Ras-responsive element binding protein 1	0.8	1 (*Pax3* and *Foxc2*) 3 (*Hoxa1*)
8.5 dpc	TEF-1 related muscle factor	0.84	1 (*Txndr2* and *Cldn5*)
	c-Rel	0.91	1 (*Txndr2*) 2 (*Cldn5*)
	Yin and Yang 1 repressor sites	0.94	1 (*Txndr2* and *Cldn5*)
14.5 dpc	Muscle TATA box	0.84	1 (*Mrpl40* and *Ranbp1*)

The value near the transcription factor indicates the obtained threshold level; numbers in the third column indicate how many times the TFBS was found in the aligned 5 kb upstream region of the co-regulated genes.

threshold of 0.80. With this threshold, we identified 10 conserved consensus sequences for transcription factors common to the downregulated genes at 4.5 dpc (*Pax3*, *Hoxa1* and *Foxc2*), 3 TFBSs common to the upregulated genes at 8.5 dpc (*Txndr2* and *Cldn5*) and 1 TFBSs common to the upregulated genes at 14.5 dpc (*Mrpl40* and *Ranbp1*) (Table 3). No common TFBSs were found among the other co-regulated genes.

4. Discussion

Regulation of gene expression during embryogenesis and development is a crucial clue for a normal anatomy and physiology (Siddiqui et al., 2005). Very little is known regarding factors that influence and regulate this expression. Similarly, there is little information available concerning the effects of a coordinate expression of a group of functionally related genes. Zhang et al. (2004) demonstrated that distinct and coordinate expression of a group of functionally related genes implies an underlying pathway-specific transcriptional regulatory mechanism. The identification of such mechanisms could represent a step towards the delineation of the features of abnormalities observed in complex developmental defects including 22q11DS.

22q11DS is attributable to a deletion of about 3 Mb detected in over 90% of patients. This typically deleted region contains over 40 genes (Paylor and Lindsay, 2006). Deletion mapping in patients led to the conclusion that the hemizygosity of different subsegments within chromosomal band 22q11.2 may be sufficient to cause the phenotype, but, paradoxically, none of these segments needs to be deleted for the expression of the phenotype (Baldini, 2004). Therefore, the existence of a "classic" 'DGS critical region', defined as a deleted region necessary and sufficient to cause the characteristic phenotype, is not supported. This conclusion is based on the fact that a very small group of patients carry non-overlapping deletions (Amati et al., 1999). A possible explanation for this observation is that there are discrete factors or sets of factors that control a set of coordinated and co-regulated genes (Vitelli et al., 2002; Stalmans et al., 2003; Guris et al., 2006). This could also explain the overlapping phenotype of undeleted patients exposed to specific teratogen, like retinoic acid.

With the aim to analyse the regulation of the expression of genes orthologous to human 22q11 during mouse embryogenesis, we constructed a low-density microarray containing 22q11 mapping genes and a subset of other genes considered "modifier genes" of the phenotype of 22q11del patients. This oligo-array is highly specific and selective and is able to detect alteration in expression levels in a selected group of genes. We applied this oligo-array to RNA obtained from mouse embryos at different developmental stages (from 4.5 dpc to 14.5 dpc; corresponding to the pharyngeal development). Samples from 4.5 dpc to 9.5 dpc include maternal and extra-embryonic tissues, however these "contaminant" tissues contribute for a minimum part to the total RNA analysed; in fact it is known that the formation of a 2-cell mouse embryo marks the transition from maternal gene to zygotic gene dependence. Maternal mRNA degradation is triggered by meiotic maturation and ~90% completed in 2-cell embryos although maternal protein synthesis continues into the 8-cells stage (Nothias et al., 1995). So the expression data we obtained at these developmental stages may be considered principally derived from embryos RNA.

In this study, we identified a total of 11 genes expressed with a FC>±2 during mouse pharyngeal development (Table 2, in bold). Seven of these differentially expressed genes map in the 22q11 chromosomal region (*Stk22a*, *Usp18*, *Txnrd2*, *Cldn5*, *Comt*, *Mrpl40* and *Ranbp1*) (Table 2, in bold). Three of them are particularly involved in embryogenesis (*Pax3*, *Foxc2* and *Hoxa1*) and one is active in retinoic acid metabolism (*Crabp1*) (Table 2, in bold). To determine better the putative roles of these differentially expressed genes in a possible orchestrated process, they are discussed according to the developmental stage in which they are expressed.

4.1. Co-expressed genes during mouse pharyngeal development

At 4.5 dpc we found the underexpression of *Foxc2*, *Pax3*, and *Hoxa1* genes (Table 2, in bold). Moreover these genes are expressed during all the developmental stages we analysed (Fig. 1C, D and E). *Pax3* and *Hoxa1* share the same expression

profile. In fact, they are expressed at all the developmental stages analysed with a level comprised between ±2. Moreover, both have a decrease of expression when we compare 4.5 dpc to 6.5 dpc ($FC_{Pax3}=-2.09$, Fig. 1D; $FC_{Hoxa1}=-2.28$, Fig. 1E); that is, they are less expressed at 4.5 dpc than at 6.5 dpc.

Pax3 (Paired box gene 3) encodes for a transcription factor expressed in the developing embryo and is a critical factor for the adequate formation of the mammalian nervous, cardiovascular and muscular systems (Goulding et al., 1991) Interestingly, our time-course analysis revealed that *Pax3* expression is lower at 4.5 dpc after which its expression remains constant (Fig. 1D). So, our data suggest that a continuous expression of *Pax3* is required for a normal development, even if at the beginning of development, *Pax3* expression is lower.

Hoxa1 (Homeobox A1) is a member of a transcription factor family which is tightly expressed during development. *Hoxa1*, together with *Hoxb1*, is required for the migration of neural crest cells into the second pharyngeal pouch. If both genes are knocked-out from mice, the second pouch-derived structures fail to form (Gavalas et al., 1998; Studer et al., 1998). Recently, *HOXA1* mutations have been found in patients with Bosley–Salih–Alorainy syndrome (BSAS) (Tischfield et al., 2005). This syndrome is characterized by horizontal gaze abnormalities, deafness, facial weakness, hypoventilation, vascular malformations of the internal carotid arteries and cardiac outflow tract, mental retardation and autism spectrum disorder. Interestingly, *Hoxa1* expression is regulated by retinoic acid (Pasqualetti and Rijli, 2001). We revealed a constant level of *Hoxa1* expression during all the phases of the pharyngeal development, suggesting that its expression level must be tightly regulated during development (Fig. 1E).

Foxc2 (Forkhead 2) gene encodes for a transcription factor expressed in the forming somites, in head mesoderm and in endothelial and mesenchymal cells of the developing heart and blood vessels. *Foxc2* null mutants die pre- and perinatally with skeletal, genitourinary and cardiovascular defects (Iida et al., 1997; Winnier et al., 1997; Kume et al., 2001). Mutations in *FOXC2* cause the human lymphedema-distichiasis syndrome (OMIM, 153400), an autosomal dominant disorder characterized principally by lymphedema of the limbs and double rows of eyelashes. One of the complications of this disorder may include cardiac defects suggesting that *FOXC2* is a gene with pleiotropic effects acting during development. Here, we demonstrate that *Foxc2* is expressed at all the developmental stages analysed (from 4.5 to 14.5 dpc) and that its expression level remains constant except in the stages from 9.5 dpc to 11.5 dpc when it decreases ($FC=-2.86$; Fig. 1C). These developmental stages correspond to a 20–24 days human embryo and to a critical stage for *Tbx1* expression (Xu et al., 2005). In fact, it is known that *Foxc2* binds and activates *Tbx1* in head mesenchyme and during arch aortic formation (Yamagishi et al., 2003). Moreover, at 9.5 dpc *Foxc2* is expressed, even if in a weak level, in the heart and in the outflow tract (Kanzaki-Katoa et al., 2005). Therefore, it is possible that a perturbation of *Foxc2* expression patterns during development, and in particular during the transition from 9.5 to 11.5 dpc, may influence the expressivity and penetrance of 22q11DS phenotype.

At 6.5 dpc three genes showed a fold change level >±2, *Stk22a* (*Tsk1*), *Usp18* and *Txnrd2*. All of them are overexpressed (Table 2, in bold). *Tsk1* gene maps in the typically deleted region on chromosome 22q11 and encodes for a serine–threonine kinase which is prevalently expressed in mouse testis (Goldmuntz et al., 1997). Mice homozygous for a deletion of 150 kb, including seven genes one of which is *Tsk1* (Kimber et al., 1999), die soon after implantation. This indicates that this deleted region contains genes which are essential for early post-implantation embryonic development. On this basis, we suggest that the increased expression of *Tsk1* at 6.5 dpc (Table 2, FC= +2.45), may be crucial during early embryogenesis. *Usp18* (Ubiquitin specific protease 18) expression is increased at 6.5 and 7.5 dpc (Table 2, in bold). *USP18*, also known as *UBP43* has been described as a specific protease that removes ISG15, a conjugated ubiquitin-like modifier, from target proteins (Malakhov et al., 2002). Previous studies from several laboratories have linked ISG15 and ISGylation to different biological activities (Martensen and Justesen, 2004; Ritchie and Zhang, 2004). A recent paper demonstrated that *UBP43* protease activity might not be as specific for ISG15 conjugates, and it could also cleave other ubiquitin or UBL conjugates in vivo (Knobeloch et al., 2005). Alternatively, *UBP43* might have another unknown biological function, which is probably crucial during development. *Txnrd2* (mitochondrial thioredoxin reductase) is overexpressed at 6.5, 8.5 and 9.5 dpc (Table 2, in bold). Thioredoxins (Txn) are small redox-reactive proteins that regulate many cellular processes (Arner and Holmgren, 2000). Our expression data agree with the evidence that *Txnrd2* is also essential for embryonic development. In fact, homozygous mutant embryos do not survive to birth and die after implantation at Theiler stage 15/16 (9.5–10 dpc). The homozygous mutant embryos display an open anterior neural tube and show massively increased apoptosis at 10.5 days postcoitus and are not present by 12.5 dpc. The timing of the embryonic lethality coincides with the maturation of the mitochondria, since they begin oxidative phosphorylation during this stage of embryogenesis (Conrad et al., 2004; Nonn et al., 2003). Analysis of heterozygous mice which are fertile and have no discernible phenotype visible by external observation, despite having decreased Txnrd-2 mRNA and protein, seemed to demonstrate that it is not a dose-sensitive gene (Nonn et al., 2003). Nevertheless, a recent paper found *Txnrd2* downregulated in the pharyngeal region of 9.5 dpc Df1/+; Tbx1+/− mouse embryos (Ivins et al., 2005). We found *Txnrd2* overexpressed in different developmental stages in normal mice when we compare it with the reference RNA (pooled 18.5 embryos) (Table 2, in bold); however all these data suggest that a precise dosage of *Txnrd2* gene product is important for normal development. *Txnrd2* gene can, therefore, be considered a possible modifier gene of the 22q11DS phenotype.

At 7.5 dpc, only one gene, *Usp18*, showed an expression level >±2 (Table 2). This gene was discussed over in the text (6.5 dpc).

At 8.5 dpc, *Txndr2* and *Cldn5* have an expression level higher than +2 (Table 2). *Txndr2* was discussed over in the text

(6.5 dpc). *Cldn5* (Claudin 5) maps within the TDR (Sirotkin et al., 1997) and encodes for a transmembrane protein reported to be primarily present in tight junctions of endothelial cells of all segments of blood vessels in the foetal brain (Morita et al., 1999). *Cldn5* is considered a candidate for schizophrenia susceptibility (Sun et al., 2004). More recently, the down-regulation of Claudin 5 in mouse models of muscular dystrophy and cardiomyopathy has been reported, suggesting that a correct dose of *Cldn5* may be determinant for normal heart development (Sanford et al., 2005). Our results may confirm this hypothesis, since we found a *Cldn5* overexpression at 8.5 dpc, which is a crucial developmental stage for heart morphogenesis.

At 9.5 dpc *Crabp1* and *Txndr2* are overexpressed (Table 2, in bold). *Crabp1* (cellular retinoic acid binding protein I), encodes for a cytosolic retinoic acid binding protein with a great affinity for RA (Chytil and Ong, 1979). Interestingly, F9 cells which overexpressed *CRABPI*, have a significant reduction of RA-induced differentiation and RA-induced expression of *RARβ* (Boylan and Gudas, 1991). This may implicate that for a normal pharyngeal development, *Crabp1* expression is crucial. Consequently, it is also important for a controlled reduction of RA-induced differentiation. All these data, together with the knowledge that either a deficiency or an excess of vitamin A (and its active metabolite retinoic acid) is detrimental to pharyngeal development and causes a DGS phenotype in humans and rodents (Mulder et al., 2000; Niederreither et al., 2003; Vermot et al., 2003; Cipollone et al., 2006), indicate that *Crabp1* may play an important role in modulating the penetrance of clinical symptoms in del22q11 patients.

At 11.5 dpc, *Comt* is underexpressed (Table 2, in bold). *Comt*, (catechol-*O*-methyltransferase) catalyses the methylation of catechols, such as dopamine, norepinephrine, and catecholoestrogens (Männistö and Kaakkola, 1999; Weinshilboum et al., 1999). *COMT* is expressed primarily in neurons, and is much more abundant in the prefrontal cortex and hippocampus than in striatum or in brainstem dopamine neurons (Männistö and Kaakkola, 1999). Maynard et al. (2003) founded that *Comt* is expressed in whole embryos at 10 and 14 dpc; we demonstrate that *Comt* is underexpressed (FC=−2.29, Table 2) at 11.5 dpc. Our data demonstrates that the expression level of *Comt* gene is lower at 11.5 dpc compared to the reference RNA (pooled 18.5 dpc embryos) and so that its modulation is important for a normal embryo development. Interestingly, Paterlini et al. (2005) demonstrated that *Comt* is upregulated in the frontal cortex of a KO mouse for the *Prodh* gene, another 22q11 gene, suggesting a possible interaction among them.

At 14.5 dpc, *Mrpl40* and *Ranbp1* are the two co-expressed genes (Table 2, in bold). *Mrpl40* (mitochondrial large ribosomal subunit 40) is overexpressed at 14.5 dpc (FC=+2.34, Table 2) when we compared its expression level to the reference RNA (pooled 18.5 dpc embryos) and it is also one of the two 22q11 genes which is constantly expressed during pharyngeal development (Fig. 1B). Its expression pattern is constant throughout the development stages from 4.5 dpc to 9.5 dpc. After this, there is a decrease (11.5 dpc), followed by a higher expression level (14.5 dpc). Also Maynard et al. (2003) found that *Mrpl40* is expressed in 14 dpc embryos; our time-course analysis demonstrates that the expression level of *Mrpl40* at 18.5 dpc (the end of embryogeneis) is lower than at 14.5 dpc. *Mrpl40* was isolated from the commonly deleted region on chromosome 22q11 (Funke et al., 1998) and encodes a 206 amino acid-long protein that contains two consensus sequences for nuclear localization signals and a putative leucine zipper near the N terminus. Accardi et al. (2004), provided evidence which showed that the product of this gene stabilizes the mtDNA in yeast strains defective for *Mmf1* gene. Further studies are required to determine if *Mrpl40* is a dose-dependent gene and to determine if its misregulation may contribute to the phenotype of del22q11 patients.

Ranbp1 (RAN binding protein 1) is overexpressed at 14.5 dpc (FC=+2.13, Table 2). The time-course analysis revealed that *Ranbp1* RNA level is constant during all the developmental stages except when we compare its expression level at 14.5 dpc vs 18. dpc, when we notice a clear increase in the expression from 14.5 dpc to 18.5 dpc (Fig. 1A). The role of Ranbp1 is not fully understood. In fact, this gene encodes for a 201-amino acid protein that binds to RAN complexed with GTP (Bischoff et al., 1995). In mammalian cells, an overexpression of *Ranbp1* interferes with crucial factor(s) that control structural and dynamic features of centrosomes during mitosis and contributes to uncover novel mitotic functions downstream of the Ran network (Di Fiore et al., 2003). A recent paper demonstrated that this network is essential for the self-organization of microtubules into a bipolar spindle (Caudron et al., 2005). As we have already indicated for *Mrpl40*, our data demonstrate that *Ranbp1* expression is highly modulated during pharyngeal development. This indicates that whatever perturbation of this gene, may have important phenotypic consequences. For these reasons, we consider *Ranbp1* as a candidate gene for a modifier role of the complex 22q11DS phenotype.

All the 11 co-regulated genes we identified in this study are massively studied and we found a good agreement between our expression data and those obtained from literature and from the Mouse Genome Informatics (MGI, http://www.informatics.jax.org). In particular there is a good comparison among the temporal expression data; this is particularly evident for the late developmental stages (from 8.5 dpc to 18.5 dpc). As regards *Foxc2*, *Pax3*, *Hoxa1*, *Tsk1*, *Usp18* and *Txnrd2* expression data, our results are original and they represent the first evidence of the expression level of these genes in the preliminary phases of mouse embryogenesis.

4.2. Definition of common TBFSs in co-regulated 22q11DS-chip genes

At the most basic level, any particular cell state can be defined by a gene expression profile and therefore by the set of transcription factors that determine its phenotype. For this reason, after the establishment of the 22q11 gene expression pattern during pharyngeal development, we analysed the promoter region of the co-regulated genes with the aim of identifying common transcription factor binding sites and consequently new genes potentially involved in modifying the

complex 22q11DS phenotype. Using a bioinformatic approach, we failed to find TFBSs in co-regulated genes at 6.5, 7.5, 9.5 and 11.5 dpc. However, we were able to detect 10 conserved TFBSs in the promoter region of underexpressed genes at 4.5 dpc (Table 3). Among these common TFBSs, of interest is the Kruppel-like zinc finger protein 219 (*Znf219*). In fact, *Znf219*, is particularly expressed in the inner cell mass of the blastocyst (Yoshikawa et al., 2006). This temporal expression might confirm a functional role of *Znf219* in the co-regulation of *Foxc2*, *Pax3* and *Hoxa1* genes, in 4.5 dpc embryos (Table 3). Also *Gsh-2*, *Nkx2.5* and *Foxf2* are interesting, even if not for their expression timing, for their expression pattern. In fact, the homeobox *Gsh-2* (genomic screened homeobox-2), that shows the highest threshold (Table 3) is a transcription factor expressed in the developing central nervous system (Hsieh-Li et al., 1995). Homozygous mutants uniformly failed to survive more than one day following birth (Szucsik et al., 1997). Interestingly, *Gsh2* is required for normal retinoid production and signaling within the ventral telencephalon (Waclaw et al., 2004). Due to its expression pattern, *Gsh-2* should be studied as a potential modifier gene for the psychiatric disorders of del22q11 patients. The homeobox factor cardiac specific *Nkx2.5/Csx* is expressed only in the heart and in heart-progenitor cells from a very early developmental stage (Akazawa and Komuro, 2005). Moreover, targeted disruption of *Nkx-2.5/Csx* expression in murine embryos results in embryonic lethality due to abnormal looping of the primary heart tube (Lyons et al., 1995). Finally, it is known that *Nkx-2.5/Csx* mutations are found in patients with atrial septum defects and atrioventricular conduction delay (Schott et al., 1998). Interestingly, a recent paper demonstrated that Nkx2.5 interacts with Tbx1 and both proteins are responsible for the regulation of cardiac morphogenesis in the secondary heart field (Nowotschin et al., 2006). So, these data addressed the attention to *Nkx2.5* as a potential modifier gene of 22q11DS phenotype. Finally, the forkhead transcription factor *Foxf2*, that is a mammalian transcriptional activator that binds DNA as a monomer through its forkhead domain, is expressed in derivatives of the splanchnic mesoderm, i.e., the mesenchyme of organs derived from the primitive gut. In addition, *Foxf2* is also expressed in limbs and the central nervous system. Interestingly, the only reported defect in *Foxf2* null embryos is cleft palate (Ormestad et al., 2004). Since cleft palate is one of the common defects of 22q11del patients, *Foxf2* may be investigated in patients as modifier genes of the phenotype.

At 8.5 dpc, we found three common TFBSs in the promoter region of the co-regulated genes; two of them had a score above 0.9, *Yy1* and *c-Rel* (Table 3). The transcription factor *Yy1* (Yin and Yang 1) is a versatile factor, being a negative regulator in some systems and a positive regulator in others. Constitutive ablation of the *Yy1* transcription factor in mice results in peri-implantation lethality. These observations strongly suggest that *Yy1* play important additional roles during late embryogenesis (Donohoe et al., 1999; Affar el et al., 2006). Interestingly, *Yy1* mRNA is ubiquitously expressed at E7.5, E8.5, E9.5, and E12.5 with a relatively elevated expression in the ectoplacental cone, somites, limb bud, and tail tip (Donohoe et al., 1999). The timing expression of *Yy1* would demonstrate that this transcription factor might have a functional role in the overexpression of *Txndr2* and *Cldn5* genes (Table 1).

The transcription factor *c-rel* is expressed first in the mesoderm-derived hematopoietic cells of the liver and later also in other hematopoietic tissues such as the thymus and spleen. This correlation between *c-rel* expression and places of hematopoietic infiltration is conserved in the postnatal period, with expression of *c-rel* mRNA in the medullary region of the thymus and in splenic B cell areas, including the marginal zone and the outer region of the periarterial sheath (Carrasco et al., 1994). The expression pattern of *c-rel* during mouse embryogenesis, renders it a potential modifier gene for the thymic phenotype of del22q11 patients.

Finally at 14.5 dpc, we found only one common TFBS in the promoter region of *Mrpl40* and *Ranbp1*. The common TFBS is a TATA box, which is the sequence recognized by TBP (TATA-binding protein) which together with TFIIB and RNA polymerase II, constitutes the basal transcriptional machinery of eukaryotic mRNAs. Computational analysis of metazoan genomes suggests that the prevalence of the TATA box has been overestimated in the past and that the majority of human genes are TATA-less.

After this bioinformatic analysis of common human and mouse promoter region, we identified three novel potential modifier gene (*Gsh-2*, *Nkx2.5* and *Yy1*) targets for a mutational screening analysis of del22q11 patients.

In conclusion, this report contains a specific and selective analysis of dynamic gene expression during mouse development. We have shown which genes were differentially expressed in specific stages of development and we have identified some candidate genes that may be related to DGS phenotype (*Nkx2.5* and *Foxc2* are examples).

We have also shown that oligonucleotides DNA microarray (DGS-chip) can represent a valid tool to improve the knowledge of the pathogenesis of 22q11DS. Further studies are underway to analyse the expression pattern revealed by the DGS-chip in mouse models of 22q11DS. It is our hope that this freely available DGS-chip will enable researchers worldwide involved in DGS to exploit further biomedical research in this interesting field.

Acknowledgements

This work was supported by a MIUR grant (Italian Ministry of University and Research) and the Italian Ministry of Health. Preliminary results of this study were presented at the Fifth International 22q11.2 deletion syndrome Conference (10–11th July 2006, Marseilles, France).

References

Accardi, R., Oxelmark, E., Jauniaux, N., de Pinto, V., Marchini, A., Tommasino, M., 2004. High levels of the mitochondrial large ribosomal subunit protein 40 prevent loss of mitochondrial DNA in null mmf1 *Saccharomyces cerevisiae* cells. Yeast 21, 539–548.

Affar el, B., et al., 2006. Essential dosage-dependent functions of the transcription factor yin yang 1 in late embryonic development and cell cycle progression. Mol. Cell. Biol. 26, 3565–3581.

Akazawa, H., Komuro, I., 2005. Cardiac transcription factor Csx/Nkx2-5: its role in cardiac development and diseases. Pharmacol. Ther. 107, 252–268.
Amati, F., et al., 1999. Atypical deletions suggest five 22q11.2 critical regions related to the DiGeorge/velo-cardio-facial syndrome. Eur. J. Hum. Genet. 7, 903–909.
Arner, E.S., Holmgren, A., 2000. Physiological functions of thioredoxin and thioredoxin reductase. Eur. J. Biochem. 267, 6102–6109.
Baldini, A., 2004. DiGeorge syndrome: an update. Curr. Opin. Cardiol. 19, 201–204.
Benjamini, Y., Hochberg, Y., 1995. Controlling the false discovery rate: a practical and powerful approach to multiple testing. J. R. Stat. Soc., Ser. B 57, 289–300.
Bischoff, F.R., Krebber, H., Smirnova, E., Dong, W., Ponstingl, H., 1995. Co-activation of RanGTPase and inhibition of GTP dissociation by Ran-GTP binding protein RanBP1. EMBO J. 14, 705–715.
Boylan, J.F., Gudas, L.J., 1991. Overexpression of the cellular retinoic acid binding protein-I (CRABP-I) results in a reduction in differentiation-specific gene expression in F9 teratocarcinoma cells. J. Cell Biol. 112, 965–979.
Carrasco, D., Weih, F., Bravo, R., 1994. Developmental expression of the mouse c-rel proto-oncogene in hematopoietic organs. Development 120, 2991–3004.
Cartharius, K., et al., 2005. MatInspector and beyond: promoter analysis based on transcription factor binding sites. Bioinformatics 21, 2933–2942.
Caudron, M., Bunt, G., Bastiaens, P., Karsenti, E., 2005. Spatial coordination of spindle assembly by chromosome-mediated signalling gradients. Science 309, 1373–1376.
Chytil, F., Ong, D.E., 1979. Cellular retinol- and retinoic acid-binding proteins in vitamin A action. Fed. Proc. 38, 2510–2514.
Cipollone, D., et al., 2006. A multiple retinoic acid antagonist induces conotruncal anomalies including transposition of the great arteries in the mouse. Cardiovasc. Pathol. 15, 194–202.
Conrad, M., et al., 2004. Essential role for mitochondrial thioredoxin reductase in hematopoiesis, heart development, and heart function. Mol. Cell. Biol. 24, 9414–9423.
Di Fiore, B., et al., 2003. Mammalian RanBP1 regulates centrosome cohesion during mitosis. J. Cell Sci. 116, 3399–3411.
Donohoe, M.E., Zhang, X., McGinnis, L., Biggers, J., Li, E., Shi, Y., 1999. Targeted disruption of mouse Yin Yang 1 transcription factor results in peri-implantation lethality. Mol. Cell. Biol. 19, 7237–7244.
Epstein, J.A., 2001. Developing models of DiGeorge syndrome. Trends Genet. 17, S13–S17.
Fang, Y., et al., 2003. A model-based analysis of microarray experimental error and normalisation. Nucleic Acids Res. 31, e96.
Farcomeni, A. Some results on the control of the false discovery rate under dependence. Scand. J. Statist., in press.
Funke, B., Puech, A., Saint-Jore, B., Pandita, R., Skoultchi, A., Morrow, B., 1998. Isolation and characterization of a human gene containing a nuclear localization signal from the critical region for velo-cardio-facial syndrome on 22q11. Genomics 53, 146–154.
Gavalas, A., Studer, M., Lumsden, A., Rijli, F.M., Krumlauf, R., Chambon, P., 1998. Hoxa1 and Hoxb1 synergize in patterning the hindbrain, cranial nerves and second pharyngeal arch. Development 125, 1123–1136.
Goldmuntz, E., Fedon, J., Roe, B., Budarf, M.L., 1997. Molecular characterization of a serine/threonine kinase in the DiGeorge minimal critical region. Gene 198, 379–386.
Goulding, M.D., Chalepakis, G., Deutsch, U., Erselius, J.R., Gruss, P., 1991. Pax-3, a novel murine DNA binding protein expressed during early neurogenesis. EMBO J. 10, 1135–1147.
Guris, D.L., Duester, G., Papaioannou, V.E., Imamoto, A., 2006. Dose-dependent interaction of Tbx1 and Crkl and locally aberrant RA signalling in a model of del22q11 syndrome. Dev. Cell 10, 81–92.
Hsieh-Li, H.M., Witte, D.P., Szucsik, J.C., Weinstein, M., Li, H., Potter, S.S., 1995. Gsh-2, a murine homeobox gene expressed in the developing brain. Mech. Dev. 50, 177–186.
Iida, K., et al., 1997. Essential roles of the winged helix transcription factor MFH-1 in aortic arch patterning and skeletogenesis. Development 124, 4627–4638.
Ivins, S., et al., 2005. Microarray analysis detects differentially expressed genes in the pharyngeal region of mice lacking Tbx1. Dev. Biol. 285, 554–569.
Jerome, L.A., Papaioannou, V.E., 2001. DiGeorge syndrome phenotype in mice mutant for the T-box gene, Tbx1. Nat. Genet. 27, 286–291.
Kanzaki-Katoa, N., et al., 2005. Roles of forkhead transcription factor Foxc2 (MFH-1) and endothelin receptor A in cardiovascular morphogenesis. Cardiovasc. Res. 65, 711–718.
Kimber, W.L., et al., 1999. Deletion of 150 kb in the minimal DiGeorge/velocardiofacial syndrome critical region in mouse. Hum. Mol. Genet. 8, 2229–2237.
Knobeloch, K.P., Utermohlen, O., Kisser, A., Prinz, M., Horak, I., 2005. Reexamination of the role of ubiquitin-like modifier ISG15 in the phenotype of UBP43-deficient mice. Mol. Cell. Biol. 25, 11030–11034.
Kume, T., Jiang, H., Topczewska, J.M., Hogan, B.L., 2001. The murine winged helix transcription factors, Foxc1 and Foxc2, are both required for cardiovascular development and somitogenesis. Genes Dev. 15, 2470–2482.
Lindsay, E.A., Baldini, A., 2001. Recovery from arterial growth delay reduces penetrance of cardiovascular defects in mice deleted for the DiGeorge syndrome region. Hum. Mol. Genet. 10, 997–1002.
Lyons, I., et al., 1995. Myogenic and morphogenetic defects in the heart tubes of murine embryos lacking the homeobox gene Nkx2-5. Genes Dev. 9, 1654–1666.
Malakhov, M.P., Malakhova, O.A., Kim, K.I., Ritchie, K.J., Zhang, D.E., 2002. UBP43 (USP18) specifically removes ISG15 from conjugated proteins. J. Biol. Chem. 277, 9976–9981.
Männistö, P.T., Kaakkola, S., 1999. Catechol-*O*-methyltransferase (COMT): biochemistry, molecular biology, pharmacology, and clinical efficacy of the new selective COMT inhibitors. Pharmacol. Rev. 51, 593–628.
Martensen, P.M., Justesen, J., 2004. Small ISGs coming forward. J. Interferon Cytokine Res. 24, 1–19.
Maynard, T.M., Haskell, G.T., Peters, A.Z., Sikich, L., Lieberman, J.A., LaMantia, A.S., 2003. A comprehensive analysis of 22q11 gene expression in the developing and adult brain. Proc. Natl. Acad. Sci. U. S. A. 100, 14433–14438.
Merscher, S., et al., 2001. TBX1 is responsible for cardiovascular defects in velo-cardio-facial/DiGeorge syndrome. Cell 104, 619–629.
Morita, K., Sasaki, H., Furuse, M., Tsukita, S., 1999. Endothelial claudin: claudin-5/TMVCF constitutes tight junction strands in endothelial cells. J. Cell Biol. 147, 185–194.
Mulder, G.B., et al., 2000. Effects of excess vitamin A on development of cranial neural crest-derived structures: a neonatal and embryologic study. Teratology 62, 214–226.
Niederreither, K., Vermot, J., Le Roux, I., Schuhbaur, B., Chambon, P., Dolle, P., 2003. The regional pattern of retinoic acid synthesis by RALDH2 is essential for the development of posterior pharyngeal arches and the enteric nervous system. Development 130, 2525–2534.
Nonn, L., Williams, R.R., Erickson, R.P., Powis, G., 2003. The absence of mitochondrial thioredoxin 2 causes massive apoptosis, exencephaly, and early embryonic lethality in homozygous mice. Mol. Cell. Biol. 23, 916–922.
Nothias, J.Y., Majumder, S., Kaneko, K.J., DePamphilis, M.L., 1995. Regulation of gene expression at the beginning of mammalian development. J. Biol. Chem. 270, 22077–22078.
Nowotschin, S., Liao, J., Gage, P.J., Epstein, J.A., Campione, M., Morrow, B.E., 2006. Tbx1 affects asymmetric cardiac morphogenesis by regulating Pitx2 in the secondary heart field. Development 133, 1565–1573.
Ormestad, M., Astorga, J., Carlsson, P., 2004. Differences in the embryonic expression patterns of mouse Foxf1 and -2 match their distinct mutant phenotypes. Dev. Dyn. 229, 328–333.
Pasqualetti, M., Rijli, F.M., 2001. Vitamin A prevents inner ear defects in mice with congenital homeobox gene deficiency. Sci. World J. 1, 916–918.
Paterlini, M., et al., 2005. Transcriptional and behavioral interaction between 22q11.2 orthologs modulates schizophrenia-related phenotypes in mice. Nat. Neurosci. 8, 1586–1594.
Paylor, R., Lindsay, E., 2006. Mouse models of 22q11 deletion syndrome. Biol. Psychiatry 59, 1172–1179.
Prescott, K., Ivins, S., Hubank, M., Lindsay, E., Baldini, A., Scambler, P., 2005. Microarray analysis of the Df1 mouse model of the 22q11 deletion syndrome. Hum. Genet. 116, 486–496.
Ritchie, K.J., Zhang, D.E., 2004. ISG15: the immunological kin of ubiquitin. Semin. Cell Dev. Biol. 15, 237–246.
Ryan, A.K., et al., 1997. Spectrum of clinical features associated with interstitial chromosome 22q11 deletions: a European collaborative study. J. Med. Genet. 34, 798–804.

Sanford, J.L., Edwards, J.D., Mays, T.A., Gong, B., Merriam, A.P., Rafael-Fortney, J.A., 2005. Claudin-5 localizes to the lateral membranes of cardiomyocytes and is altered in utrophin/dystrophin-deficient cardiomyopathic mice. J. Mol. Cell. Cardiol. 38, 323–332.

Scambler, P.J., 2000. The 22q11 deletion syndromes. Hum. Mol. Genet. 9, 2421–2426.

Scharpf, R.B., Iacobuzio-Donahue, C., Sneddon, J.B., Parmigiani, G., 2005. When should one subtract background fluorescence in two color microarrays? Technical Report 50, Department of Biostatistics, Johns Hopkins Bloomberg School of Public Health.

Schott, J.J., et al., 1998. Congenital heart disease caused by mutations in the transcription factor NKX2-5. Science 281, 108–111.

Siddiqui, A.S., et al., 2005. A mouse atlas of gene expression: large-scale digital gene expression profiles from precisely defined developing C57BL/6J mouse tissues and cells. Proc. Natl. Acad. Sci. U. S. A. 102, 18485–18490.

Sirotkin, H., et al., 1997. Identification, characterization, and precise mapping of a human gene encoding a novel membrane-spanning protein from the 22q11 region deleted in velo-cardio-facial syndrome. Genomics 42, 245–251.

Stalmans, I., et al., 2003. VEGF: a modifier of the del22q11 (DiGeorge) syndrome? Nat. Med. 9, 173–182.

Studer, M., et al., 1998. Genetic interactions between Hoxa1 and Hoxb1 reveal new roles in regulation of early hindbrain patterning. Development 125, 1025–1036.

Sun, Z.Y., et al., 2004. The CLDN5 locus may be involved in the vulnerability to schizophrenia. Eur. Psychiatr. 19, 354–357.

Szucsik, J.C., Witte, D.P., Li, H., Pixley, S.K., Small, K.M., Potter, S.S., 1997. Altered forebrain and hindbrain development in mice mutant for the Gsh-2 homeobox gene. Dev. Biol. 191, 230–242.

Tischfield, M.A., et al., 2005. Homozygous HOXA1 mutations disrupt human brainstem, inner ear, cardiovascular and cognitive development. Nat. Genet. 37, 1035–1037.

Vermot, J., Niederreither, K., Garnier, J.M., Chambon, P., Dolle, P., 2003. Decreased embryonic retinoic acid synthesis results in a DiGeorge syndrome phenotype in newborn mice. Proc. Natl. Acad. Sci. U. S. A. 100, 1763–1768.

Vitelli, F., Taddei, I., Morishima, M., Meyers, E.N., Lindsay, E.A., Baldini, A., 2002. A genetic link between Tbx1 and fibroblast growth factor signaling. Development 129, 4605–4611.

Waclaw, R.R., Wang, B., Campbell, K., 2004. The homeobox gene *Gsh2* is required for retinoid production in the embryonic mouse telencephalon. Development 131, 4013–4020.

Weinshilboum, R.M., Otterness, D.M., Szumlanski, C.L., 1999. Methylation pharmacogenetics: catechol-*O*-methyltransferase, thiopurine methyltransferase, and histamine *N*-methyltransferase. Annu. Rev. Pharmacol. Toxicol. 39, 19–52.

Winnier, G.E., Hargett, L., Hogan, B.L.M., 1997. The winged helix transcription factor MFH1 is required for proliferation and patterning of paraxial mesoderm in the mouse embryo. Genes Dev. 11, 926–940.

Xu, H., Cerrato, F., Baldini, A., 2005. Timed mutation and cell-fate mapping reveal reiterated roles of Tbx1 during embryogenesis, and a crucial function during segmentation of the pharyngeal system via regulation of endoderm expansion. Development 132, 4387–4395.

Yamagishi, H., et al., 2003. Tbx1 is regulated by tissue-specific forkhead proteins through a common Sonic hedgehog-responsive enhancer. Genes Dev. 17, 269–281.

Yang, Y.H., Dudoit, S., Luu, P., Terence, P., 2001. Speed normalization for cDNA microarray data. Proc. SPIE 4266, 141.

Yoshikawa, T., et al., 2006. High-throughput screen for genes predominantly expressed in the ICM of mouse blastocysts by whole mount in situ hybridization. Gene Expr. Patterns 6, 213–224.

Zhang, W., et al., 2004. The functional landscape of mouse gene expression. J. Biol. 3, 21.